Articles

Assembly of Hybrid Inorganic−Organic Materials from Octahedral Nb_6 Clusters and Metal Complexes

Huajun Zhou, Cynthia S. Day, and Abdessadek Lachgar*

Department of Chemistry, Wake Forest University, Winston-Salem, North Carolina 27109

Received June 22, 2004. Revised Manuscript Received August 23, 2004

The octahedral edge-bridged niobium cyano-chloride cluster $[Nb_6Cl_{12}(CN)_6]^{4-}$ and the $[Mn(salen)]^+$ metal complex have been used as building units to prepare solid-state materials with extended frameworks at room temperature through self-assembly processes. Three materials with different dimensionalities were prepared and characterized: $(Me_4N)_4[Nb_6Cl_{12}(CN)_6]\cdot 2MeOH$ (**1**) (0D), $(Me_4N)_2[Mn(salen)]_2[Nb_6Cl_{12}(CN)_6]$ (**2**) (2D), and $(Et_4N)_2[Mn(salen)(MeOH)]_2[Nb_6Cl_{12}(CN)_6]\cdot 2MeOH$ (**3**) (1D). **1** was used as cluster precursor for the preparation of **2** and **3**. The framework dimensionality seems to be affected by the size of the template-counterion used. Single-crystal X-ray analysis revealed that **1** is based on discrete $[Nb_6Cl_{12}(CN)_6]^{4-}$ separated by $(Me_4N)^+$ and MeOH molecules. **2** has a two-dimensional framework, in which each layer is formed by $[Nb_6Cl_{12}(CN)_6]^{4-}$ clusters connected through four cyanide ligands to four different $[Mn(salen)]^+$. Each manganese complex connects two clusters through Nb−CN−Mn−NC−Nb bridges, leading to the formation of anionic layers interleaved by $(Me_4N)^+$. In **3**, every cluster unit $[Nb_6Cl_{12}(CN)_6]^{4-}$ is linked to two $[Mn(salen)(MeOH)]^+$ units through two apical trans cyanide ligands, leading to the formation of trimeric units {Mn−(NC)$[Nb_6Cl_{12}(CN)_4]$(CN)−Mn}. Every trimeric unit connects to two neighboring units through hydrogen bonding between O_{MeOH} from coordinated methanol ligand and N_{CN} from two neighboring clusters, resulting in the formation of anionic chains along the crystallographic ***a*** axis $\{[Mn(salen)(MeOH)]_2[(Nb_6Cl_{12})(CN)_6]\}^{2-}$. The chains are separated by $(Et_4N)^+$ and MeOH. Magnetic properties and thermal behavior of these new hybrid inorganic−organic compounds are presented.

Introduction

The field of crystal engineering has expanded beyond its original application to organic-based materials, and became interdisciplinary in nature combining coordination chemistry, supramolecular chemistry, coordination polymers, and hybrid inorganic−organic materials.[1] The ultimate goal of crystal engineering is to use predesigned molecular or nanosize building units to prepare supramolecular species or polymeric materials with novel structural and functional properties in a predictable fashion.[2] The use of nanosize building units to prepare hybrid inorganic−organic materials has been applied to systems such as organotin−oxo clusters, organically functionalized polyoxometalates, and transition metal clusters.[3] More recently octahedral metal clusters with metal−metal bonds have been used as subunits for building structural analogues of materials built of simple mononuclear species. The use of these clusters is rationalized on the basis of their size, well-defined geometry, chemical stability, and electronic flexibility. For example, water-soluble $[Re_6Q_8(CN)_6]^{4-}$ (Q = Se, Te) metal clusters were used to prepare materials with structures that are expanded analogues of Prussian blue, and materials with vapochromic response and enhanced ion-exchange properties.[4] Here,

* To whom correspondence should be addressed. Fax: 336-758-4656. E-mail: lachgar@wfu.edu.

(1) (a) Schmidt, G. M. J. *Pure Appl. Chem.* **1971**, *27*, 647. (b) Desiraju, G. R. *Crystal Engineering: The Design of Organic Solids*; Elsevier: New York, **1989**. (c) Hagrman, P. J.; Zubieta, D. J. *Angew. Chem., Int. Ed.* **1999**, *38*, 2638. (d) Braga, D.; Grepioni, F.; Orpen, A. G., Eds. *Crystal Engineering: From Molecules and Crystals to Materials;* Kluwer Academic Publishers: Dordrecht, 1999. (e) Braga, D. *J. Chem. Soc., Dalton Trans.* **2000**, 3705. (f) Moulton, B.; Zaworotko, M. J. *Chem. Rev.* **2001**, *101*, 1629. (g) Dinolfo, P. H.; Hupp, J. T. *Chem. Mater.* **2001**, *13*, 3113. (h) Seidel, S. R.; Stang, P. J. *Acc. Chem. Res.* **2002**, *35*, 972. (i) Evans, O. W.; Lin, W. *Acc. Chem. Res.* **2002**, *35*, 511. (j) Černák, J.; Orendáč, M.; Potočňák, I.; Chomič, J.; Orendáčová, A.; Skoršepa, J.; Feher, A. *Coord. Chem. Rev.* **2002**, *224*, 51.

(2) (a) Braga, D.; Grepioni, F. *Acc. Chem. Res.* **2000**, *33*, 601. (b) Khlobystov, A. N.; Blake, A. J.; Champness, N. R.; Lemenovskii, D. A.; Majouga, A. G.; Zyk, N. V.; Schroder, M. *Coord. Chem. Rev.* **2001**, *222*, 155. (c) Holliday, B. J.; Mirkin, C. A. *Angew. Chem., Int. Ed.* **2001**, *40*, 2022.

(3) (a) Holmes, R. R. *Acc. Chem. Res.* **1989**, *22*, 190. (b) Lichtenhan, J. D. *Comments Inorg. Chem.* **1995**, *17*, 115. (c) Mazeaud, A.; Ammari, N.; Robert, F.; Thouvenot, R. *Angew. Chem., Int. Ed. Engl.* **1996**, *35*, 1961. (d) Bowes, C. L.; Huynh, W. U.; Kirkby, S. J.; Malek, A.; Ozin, G. A.; Petrov, S.; Twardowski, M.; Young, D.; Bedard, R. L.; Broach, R. *Chem. Mater.* **1996**, *8*, 2147. (e) Zhang, C.; Babonneau, F.; Bonhomme, C.; Laine, R. M.; Soles, C. L.; Hristo, H. A.; Yee, A. F. *J. Am. Chem. Soc.* **1998**, *120*, 8380. (f) Cahill, C. L.; Ko, Y.; Parise, J. B. *Chem. Mater.* **1998**, *10*, 19. (g) Ribot, F.; Eychenne-Baron, C.; Sanchez, C. *Phosphorus, Sulfur Silicon Relat. Elem.* **1999**, *150*, 41. (h) Mayer, C. R.; Herson, P.; Thouvenot, R. *Inorg. Chem.* **1999**, *38*, 6152. (i) Li, H.; Eddaoudi, M.; O'Keeffe, M.; Yaghi, O. M. *Nature* **1999**, *402*, 276. (j) Khan, M. I.; Yohannes, E.; Powell, D. *Inorg. Chem.* **1999**, *38*, 212.

10.1021/cm049007w CCC: $27.50 © 2004 American Chemical Society
Published on Web 10/26/2004

we chose to investigate the use of octahedral metal cluster $[(Nb_6Cl_{12})(CN)_6]^{4-}$ as building blocks to prepare hybrid inorganic−organic cluster-based materials for five major reasons: (*i*) the cluster represents an isotropic expansion of the mononuclear complex $[M(CN)_6]^{n-}$ in all three dimensions, which is important since the frameworks of the products tend to be interpenetrated and/or fragile if the enlargement of its components is limited to one or two dimensions;[5] (*ii*) the ability of the cyanide ligand to serve as linker between a variety of metal centers could be employed to synthesize a variety of 1D, 2D, or 3D frameworks that are interesting as ion exchangers, molecular sieves, and magnetic materials, or for gas storage;[6,7] (*iii*) compared to mononuclear complexes, metal clusters have greater electronic flexibility and thus are stable building blocks whose charges can, in principle, be changed as needed; (*iv*) the edge-bridged $[(Nb_6Cl_{12})(L)_6]^{4-}$ is easy to prepare with different ligands in axial positions and different counterions allowing the manipulation of its coordination environment, and subsequently its physical and chemical properties;[8] and (*v*) though octahedral face-capped transition metal clusters, often referred to as (6−8) type, e.g., $[M_6X_8(CN)_6]^{n-}$ (M = W, Re; X = S, Se, Te) have been used as building blocks of materials with extended frameworks,[9] the use of edge-bridged octahedral niobium clusters as building blocks is rather rare.

Among all noncovalent interactions used in inorganic crystal engineering, hydrogen bonds and coordination bonds have been successfully employed to prepare novel supramolecular structures.[10] Thus, the second building unit of the materials we aim at making consists of mononuclear metal complexes with free coordination sites, or sites occupied by good leaving groups. Among the wide variety of easily accessible metal complexes, we investigated *metal salen* complexes because *salen* ligands strongly chelate metal ions through two oxygen and two nitrogen atoms, leaving one or two free axial sites available for interactions with the cyanide ligand from the cluster units. Furthermore, *salen* complexes have remarkable catalytic properties and are able to act in a cooperative manner,[11] and cluster-based compounds containing face-capped clusters and Mn(*salen*)$^+$ have been recently reported by Kim et al.[12]

Here we report the syntheses, structures, thermal behavior, and magnetic properties of two novel extended frameworks with different dimensionality using $[Nb_6Cl_{12}(CN)_6]^{4-}$ and [Mn(*salen*)]$^+$ as building blocks. Two cluster precursors with different quaternary ammonium cations have been prepared to investigate the role played by counterions that serve as charge-compensating and structure-directing agents.

Experimental Section

General. $(Me_4N)_3[Nb_6Cl_{18}]\cdot 2MeCN$, and Mn(*salen*)$ClO_4\cdot 2H_2O$ were prepared as reported in the literature.[8i,13] Et_4NBr, $LiClO_4$, $NaClO_4$, $KClO_4$, Bu_4NCl, and PPh_4Cl were used as received from Fisher. MeCN and DMSO were used without further purification. MeOH was refluxed over sodium methoxide under N_2 atmosphere for 3 h, and stored 4 Å molecular sieves.

Synthesis. *$(Me_4N)_4[Nb_6Cl_{12}(CN)_6]\cdot 2MeOH$ (**1**).* To a solution of $(Me_4N)_3[Nb_6Cl_{18}]\cdot 2MeCN$ (0.561 g, 0.374 mmol) in 24 mL of acetonitrile was added KCN (0.5151 g, 7.91 mmol) in 18 mL of H_2O. The mixture turned green after stirring for 12 h. The solvent was removed and a solid residue was extracted with 2×50 mL of hot MeCN. A 0.376-g portion of green solid was obtained after the solvent was removed. The solid was dissolved in 45 mL of MeOH, and solid Me_4NCl (0.143 g, 1.31 mmol) was added to the solution. Dark green platelike crystals were obtained by diffusing Et_2O into the dark green solution in refrigeration to give the product (0.378 g, yield: 67%). Anal. Calcd for $C_{24}H_{56}Cl_{12}N_{10}Nb_6O_2$: C, 19.22; H, 3.77; N, 9.34%. Found: C, 18.46; H, 3.40; N, 9.60%. IR (KBr): $\nu_{CN} = 2129\ cm^{-1}$.

*$(Me_4N)_2[Mn(salen)]_2[Nb_6Cl_{12}(CN)_6]$ (**2**).* A 2-mL aliquot of a 15.0 mM methanolic solution of Mn(*salen*)$ClO_4\cdot 2H_2O$ was

(4) (a) Shores, M. P.; Beauvais, L. G.; Long, J. R. *J. Am. Chem. Soc.* **1999**, *121*, 775. (b) Beauvais, L. G.; Shores, M. P.; Long, J. R. *J. Am. Chem. Soc.* **2000**, *122*, 2763. (c) Bennett, M. V.; Shores, M. P.; Beauvais, L. G.; Long, J. R. *J. Am. Chem. Soc.* **2000**, *122*, 6664.

(5) Batten, S. R.; Robson, R. *Angew. Chem., Int. Ed.* **1998**, *37*, 1461 and references therein.

(6) (a) Mallah, S.; Thiebaut, S.; Verdaguer, M.; Viellet, P. *Science* **1993**, *262*, 1554. (b) Soma, T.; Yuge, H.; Iwamoto, T. *Angew. Chem., Int. Ed. Engl.* **1994**, *33*, 1665. (c) Ohba, M.; Okawa, H.; Ito, T.; Ohto, A. *J. Chem. Soc. Chem. Commun.* **1995**, 1545. (d) Iwamoto, T. Supramolecular Chemistry in Cyanometalate Systems. In , *Comprehensive Supramolecular Chemistry*; Lehn, J. M., Ed.; Pergamon: London, **1996**; Vol. 6, Solid State Supramolecular Chemistry, p 643. (e) Knoeppel, D. W.; Shore, S. G. *Inorg. Chem.* **1996**, *35*, 1747. (f) Zhang, H. X.; Tong, Y. X.; Chen, Z. N.; Yu, K. B.; Kang, B. S. *J. Organomet. Chem.* **2000**, *598,* 63.

(7) (a) Kämper, M.; Wagner, M.; Weiss, A. *Angew. Chem.* **1979**, *91*, 517. (b) Loos-Neskovic, C.; Fédoroff, M. *Solvent Extr. Ion Exch.* **1987**, *5*, 757. (c) Khurana, A. *Phys. Today* **1988**, *41*, 19. (d) Abrahams, B. F.; Hoskins, B. F.; Robson, R. *J. Chem. Soc. Chem. Commun.* **1990**, 60. (e) Mikeska, H. J.; Steiner, M. *Adv. Phys.* **1991**, *40*, 191, and references therein. (f) Vahrenkampf, H.; Geiss, A.; Richardson, G. N. *J. Chem. Soc., Dalton Trans.* **1997**, 3643. (g) Verdaguer, M.; Bleuzen, A.; Marvaud, V.; Vaissermann, J.; Seuleiman, M.; Desplanches, C.; Scuiller, A.; Train, C.; Garde, R.; Gelly, G.; Lomenech, C.; Rosenman, I.; Veillet, P.; Cartier, C.; Villain, F. *Coord. Chem. Rev.* **1999**, *190*, 1023.

(8) (a) Reckeweg, O.; Meyer, H. J. *Z. Naturforsch*. **1995**, *50*, 1377. (b) Reckeweg, O.; Meyer, H. J. *Z. Naturforsch*. **1997**, *212*, 234. (c) Vojnovič, M.; Antolič, S.; Kojič-Prodič, B.; Brničevič, N.; Miljakm M.; Aviani, I. *Z. Anorg. Allg. Chem.* **1997**, *623*, 1247. (c) Prokopuk, N.; Shriver, D. F. *Adv. Inorg Chem*. **1999**, *46,* 1, and references therein. (e) Vojnovic, M.; Brnicevic, N.; Basic, I.; Trojko, R.; Miljak, M.; Desnica-Frankovic, I. D. *Mater. Res. Bull.* **2001**, *36*, 211. (f) Naumov, N. G.; Cordier, S.; Perrin, C. *Angew. Chem., Int. Ed.* **2002**, *41*, 3002. (g) Naumov, N. G.; Cordier, S.; Perrin, C. *Solid State Sci*. **2003**, *5*, 1359. (h) Naumov, N. G.; Cordier, S.; Gulo, F.; Roisnel, T.; Fedorov, V. E.; Perrin, C. *Inorg. Chim. Acta* **2003**, *350*, 503. (i) Yan B. B.; Zhou H. J.; Lachgar, A. *Inorg. Chem.* **2003**, *42*, 8818.

(9) Most recent examples include: (a) Mironov, Y. V.; Fedorov, V. E.; Ijjaali, I.; Ibers, J. A. *Inorg. Chem.* **2001**, *40,* 6320. (b) Bennett, M. V.; Beauvais, L. G.; Shores, M. P.; Long, J. R. *J. Am. Chem. Soc.* **2001**, *123*, 8022. (c) Artemkina, S. B.; Naumov, N. G.; Virovets, A. V.; Gromilov, S. A.; Fenske, D.; Fedorov, V. E. *Inorg. Chem. Commun.* **2001**, *4*, 423. (d) Kim, Y.; Choi, S. K.; Park, S. M.; Nam, W.; Kim, S. J. *Inorg. Chem. Commun*. **2002**, *5*, 612. (e) Jin, S.; DiSalvo, F. J. *Chem. Mater.* **2002**, *14*, 3448. (f) Artemkina, S. B.; Naumov, N. G.; Virovets, A. V.; Oeckler, O.; Simon, A.; Erenburg, S. B.; Bausk, N. V.; Fedorov, V. E. *Eur. J. Inorg. Chem*. **2002**, 1198. (g) Selby, H. D.; Roland, B. K.; Carducci, M. D.; Zheng, Z. *Inorg. Chem.* **2003**, *42*, 1656.

(10) (a) Braga, D.; Grepioni, F.; Desiraju, G. R. *Chem. Rev.* **1998**, *98*, 1375. (b) Braga, D.; Grepioni, F. *Acc. Chem. Res.* **2000**, *33*, 601. (c) Kim, J. Y.; Norquist, A. J.; O'Hare, D. *Chem. Mater.* **2003**, *15*, 1970. (d) Woodward, J. D.; Backov, R., Abboud, K. A.; Ohnuki, H.; Meisel, M. W.; Talham, D. R. *Polyhedron* **2003**, *22*, 2821. (e) Abrahams, B. F.; Moylan, M.; Orchard, S. D.; Robson, R. *CrystEngComm* **2003**, *5*, 313. (f) Kabir, M. K.; Tobita, H.; Matsuo, H.; Nagayoshi, K.; Yamada, K.; Adachi, K.; Sugiyama, Y.; Kitagawa, S.; Kawata, S. *Cryst. Growth Des.* **2003**, *3*, 791.

(11) (a) Hansen, K. B.; Leighton, J. L.; Jacobsen, N. E. *J. Am. Chem. Soc.* **1996**, *118*, 10924. (b) Konsler, R. G.; Karl, J.; Jacobsen, N. E. *J. Am. Chem. Soc.* **1998**, *120*, 10780. (c) Annis, D. A.; Jacobsen, N. E. *J. Am. Chem. Soc.* **1999**, *121*, 4147. (d) Belokon, Y. N.; Caveda-Cepas, S.; Green, B.; Ikonnikov, N. S.; Krustalev, V. N.; Larichev, V. S.; Moscalenko, M. A.; North, M.; Orizu, L.; Tararov, V. I.; Tasinazzo, M.; Timofeeva, G. I.; Yashkina, V. *J. Am. Chem. Soc.* **1999**, *121*, 3968. (e) Ready, J. M.; Jacobsen, N. E. *J. Am. Chem. Soc.* **2001**, *123*, 2687.

(12) (a) Kim, Y.; Park, S. M.; Nam, W.; Kim, S. J. *Chem. Commun*. **2001**, 1470. (b) Kim, Y.; Park, S. M.; Kim, S. J. *Inorg. Chem. Commun*. **2002**, *5*, 592.

(13) Li, H.; Zhong, Z. J.; Duan, C.; You, X.; Mak, T. C. W.; Wu, B. *J. Coord. Chem.* **1997**, *41*, 183.

layered with 2 mL of 6.0 mM methanolic solution of $(Me_4N)_4[Nb_6Cl_{12}(CN)_6]\cdot 2MeOH$ in a narrow-diameter glass tube (i.d. 8 mm, $l = 12$ cm). Black platelike crystals were obtained within 2 days. The crystals were collected by filtration, washed with H_2O (5 × 3 mL), MeOH (2 × 3 mL), and Et_2O (2 × 3 mL), and dried under vacuum to get the product (13.6 mg, yield: 59%). Anal. Calcd for $C_{46}H_{52}Cl_{12}Mn_2N_{12}Nb_6O_4$: C, 28.63; H, 2.72; N, 8.71%. Found: C, 27.68; H, 2.74; N, 8.42%. IR (KBr): $\nu_{CN} = 2134$ cm^{-1}.

*$(Et_4N)_2[Mn(salen)(MeOH)]_2[Nb_6Cl_{12}(CN)_6]\cdot 2MeOH$ (**3**).* First a metathesis reaction was performed to prepare the precursor $(Et_4N)_4[Nb_6Cl_{12}(CN)_6]$. Upon addition of Et_4NBr (0.236 g, 1.123 mmol) to a solution of $(Me_4N)_4[Nb_6Cl_{12}(CN)_6]\cdot 2MeOH$ (0.2533 g, 0.169 mmol) in 20 mL of water, green precipitate formed immediately. The reaction mixture was stirred for 1 h, then the solid was collected by filtration, washed with water (5 × 5 mL), and dried under vacuum to give 0.228 g of product. The solid thus obtained was dissolved in 25 mL of MeOH to give dark green solution. A 2-mL portion of the dark green solution was layered on top of 2 mL of methanolic solution of 30.0 mM $[Mn(salen)]ClO_4\cdot 2H_2O$ in a narrow-diameter silica tube (i.d. 7 mm, $l = 12$ cm). Black blocklike crystals were obtained after 2 days. The crystals were collected by filtration, washed with MeOH (5 × 3 mL) and Et_2O (5 × 3 mL) to get dark brown product (17.2 mg, yield: 59%). Anal. Calcd for $C_{58}H_{84}Cl_{12}Mn_2N_{12}Nb_6O_8$: C, 32.10; H, 3.91; N, 7.74%. Found: C, 30.10; H, 3.79; N, 7.65% (the relatively large difference between calculated and found is probably due to solvent loss). IR (KBr): $\nu_{CN} = 2131$ cm^{-1}.

X-ray Structure Determination. *$(Me_4N)_4[Nb_6Cl_{12}(CN)_6]\cdot 2MeOH$ (**1**).* A dark green platelike crystal was selected, coated with Paratone oil, and mounted on quartz fibers for single-crystal X-ray analysis. Intensity data were collected at 193 (2) K on a Bruker SMART APEX CCD area detector system equipped with a graphite monochromator and a Mo Kα fine-focus sealed tube ($\lambda = 0.71073$ Å). Data were integrated using the Bruker SAINT software and corrected using SADABS program.[14] The structure was solved and refined in the space group *Cmca* (No. 64), $Z = 4$ for the formula unit $C_{24}H_{56}Cl_{12}N_{10}Nb_6O_2$ using the Bruker SHELXTL (Version 6.1) software package.[15] The structural model incorporated anisotropic thermal parameters for all (nonsolvent) non-hydrogen atoms and isotropic thermal parameters for all included hydrogen atoms. The final anisotropic full-matrix least-squares refinement on F^2 with 133 variables converged to $R_1 = 4.82\%$ for observed data and $wR_2 = 12.7\%$ for all data. The methyl groups of the two $(Me_4N)^+$ cations (C3, C4, C5, C6, C7, and their hydrogen atoms) were refined as rigid rotors (using idealized sp^3-hybridized geometry and C−H bond length of 0.98 Å). On the basis of residual electron density (the highest difference peak was 0.674e$^-$/Å^3) in the difference Fourier map, a disordered MeOH solvent molecule was included in the structural model. Attempts to model the MeOH molecule were unsuccessful (the distance between C8 and O1 is 1.89(3) Å) and 1/2 occupancy isotropic oxygen and carbon atoms were therefore placed at the positions reported for O1 and C8. The hydrogen atoms on the disordered solvent molecule were not included in the structural model.

*$(Me_4N)_2[Mn(salen)]_2[Nb_6Cl_{12}(CN)_6]$ (**2**).* A lustrous diamond-shaped platelike crystal of **2** with approximate dimensions 0.05 × 0.20 × 0.25 mm, was selected and attached to quartz fibers for single-crystal X-ray analysis. Intensity data were measured at 296(2) K on a Bruker SMART APEX CCD area detector system. The integration of the data using an orthorhombic cell yielded a total of 81 035 reflections to a maximum θ angle of 23.26° (0.80 Å resolution), of which 5028 were independent (redundancy 16.1), and 4192 (83.4%) were greater than $2\sigma(F^2)$. The final cell constants of $a = 23.151(1)$ Å, $b = 13.014(1)$ Å, $c = 23.201(1)$ Å, and $V = 6990.2(7)$ Å^3, are based upon the refinement of the centroids of 8598 reflections above 20 $\sigma(I)$ with $4.71° < 2\theta < 51.05°$. Analysis of the data showed negligible decay during data collection. Data were corrected for absorption effects using the multiscan technique (SADABS). The calculated minimum and maximum transmission coefficients (based on crystal size) are 0.6616 and 0.9153. The structure was solved and refined in the space group $Pbca-D_{2h}^{15}$ (No. 61), with $Z = 4$ using the Bruker SHELXTL (Version 6.1) software package. The final anisotropic full-matrix least-squares refinement on F^2 with 393 variables converged to $R_1 = 0.027\%$, for observed data and $wR_2 = 0.070$ for all data. The largest residual peak on the final difference electron density synthesis was 0.875e$^-$/Å^3 and the largest hole was −0.352 e$^-$/Å^3.

*$(Et_4N)_2[Mn(salen)(MeOH)]_2[Nb_6Cl_{12}(CN)_6]\cdot 2MeOH$ (**3**).* A Black blocklike single crystal of **3** with approximate size 0.20 × 0.20 × 0.15 mm was removed from the mother solution, coated with Paratone oil, and quickly transferred to the low-temperature nitrogen stream of the diffractometer. After a quick optical alignment data were collected at 213 (2) K. **3** was found to crystallize in the monoclinic system, space group $P2_1/c$ (No. 14) with $a = 13.227(1)$ Å, $b = 21.800(2)$ Å, $c = 13.781(1)$ Å, $\beta = 93.648(6)°$, $V = 3965.7(5)$ Å^3, and $Z = 2$. A total of 13 116 absorption-corrected reflections with $2\theta < 58.7°$ were collected on a Bruker AXS P4 diffractometer using ω scans and graphite-monochromated Mo Kα ($\lambda = 0.71073$) radiation. The structural parameters have been refined to convergence {$R_1 = 0.0605$ and $wR_2 = 0.0862$ for all 10 883 unique reflections} using counter-weighted full-matrix least-squares techniques. The structural model incorporated anisotropic thermal parameters for all nonhydrogen atoms and isotropic thermal parameters for all included hydrogen. Hydrogen atoms of the ammonium ion were omitted due to countercations disorder, and hydrogen of the solvent could not be located. X-ray crystallographic data are summarized in Table 1.

Magnetic Susceptibility. Magnetic susceptibility data for **2** were measured using a Quantum Design MPMS XL SQUID magnetometer. 37.9-mg of loose crystals of **2** was placed into a white acetal rod with threaded male and female ends. Magnetization of both the empty and filled sample holder was measured in the temperature range 2−300 K at an applied field of 5 kG. The data were corrected for the diamagnetic contributions of the sample holder.

Other Physical Measurements. Thermogravimetric analyses were performed on a 22.86-mg sample of **2** under a flow of nitrogen (40 mL/min) at a ramp rate of 5 °C/min, using a Perkin-Elmer Pyris 1 TGA system. Infrared spectra were recorded on a Mattson Infinity System FTIR spectrometer. X-ray powder diffraction data were collected on an INEL CPS 120 powder diffractometer equipped with position-sensitive detector at the rate of 0.02°/min.

Results and Discussion

Synthesis. The layering of methanolic solutions of $(Me_4N)_4[Nb_6Cl_{12}(CN)_6]\cdot 2MeOH$ (**1**) and $Mn(salen)ClO_4\cdot 2H_2O$ led to the formation of crystalline $(Me_4N)_2[Mn(salen)]_2[Nb_6Cl_{12}(CN)_6]$ (**2**). Mixing the two solutions together led to the immediate formation of poorly crystalline precipitate that could not be identified by powder XRD. However, elemental analysis of the powder agreed with that obtained for the crystalline phase obtained through the layering method. The reported procedure is optimal for the preparation of good quality crystals of **2**, however, the formation of **2** is not affected by changes in reactants concentrations as long as the concentration ratio $[Mn(salen)]^+/[Nb_6Cl_{12}(CN)_6]^{4-}$ is larger than 1. Compound **2** can also be obtained by using MeCN as solvent, indicating that the formation of **2** is independent of both concentration and solvents. Compound **2** was found to be soluble in DMSO to form a dark brown solution that was not further characterized. In contrast to **2**, the concentrations of both cluster

(14) Bruker. *SMART* version 5.625, *SAINT* version 6.02a, and *SADABS* version 2.03; Bruker AXS Inc.: Madison, WI, 2001.

(15) Sheldrick, G. M. *SHELXTL*, version 6.12; Bruker AXS Inc.: Madison, WI.

Table 1. Crystal Data and Structure Refinements for $(Me_4N)_4[Nb_6Cl_{12}(CN)_6]\cdot 2MeOH$ (1), $(Me_4N)_2[Mn(salen)]_2[Nb_6Cl_{12}(CN)_6]$ (2), and $(Et_4N)_2[Mn(salen)(MeOH)]_2[Nb_6Cl_{12}(CN)_6]\cdot 2MeOH$ (3)

	1	2	3
formula	$C_{24}H_{56}Cl_{12}N_{10}Nb_6O_2$	$C_{46}H_{52}Cl_{12}Mn_2N_{12}Nb_6O_4$	$C_{58}H_{84}Cl_{12}Mn_2N_{12}Nb_6O_8$
fw (g/mol)	1499.65	1929.74	2170.11
T, K	193	296	213
crystal system	orthorhombic	orthorhombic	monoclinic
space group	*Cmca*	*Pbca*	*P*2(1)/*c*
a (Å)	14.086(3)	23.151(1)	13.227(1)
b (Å)	20.057(4)	13.014(1)	21.800(2)
c (Å)	20.938(4)	23.201(1)	13.781(1)
β (deg)			93.648(6)
V (Å^3)	5915(2)	6990.2(7)	3965.7(5)
Z	4	4	2
ρ_{calcd} (g·cm^{-3})	1.684	1.833	1.817
μ (mm^{-1})	1.696	1.802	1.600
λ, Å	0.71073	0.71073	0.71073
R_1[a]	0.048	0.027	0.038
wR_2[b,c]	0.127	0.070	0.086

[a] $R_1 = \Sigma||F_0| - |F_c||/\Sigma|F_0|$. [b] $wR_2 = [\Sigma[w(F_o^2 - F_c^2)^2]/\Sigma[(wF_o^2)^2]]^{1/2}$. [c] $w^{-1} = \sigma^2(F_0^2) + (0.0101P)^2$ ($P = (\max(F_0^2,0) + 2F_c^2)/3$).

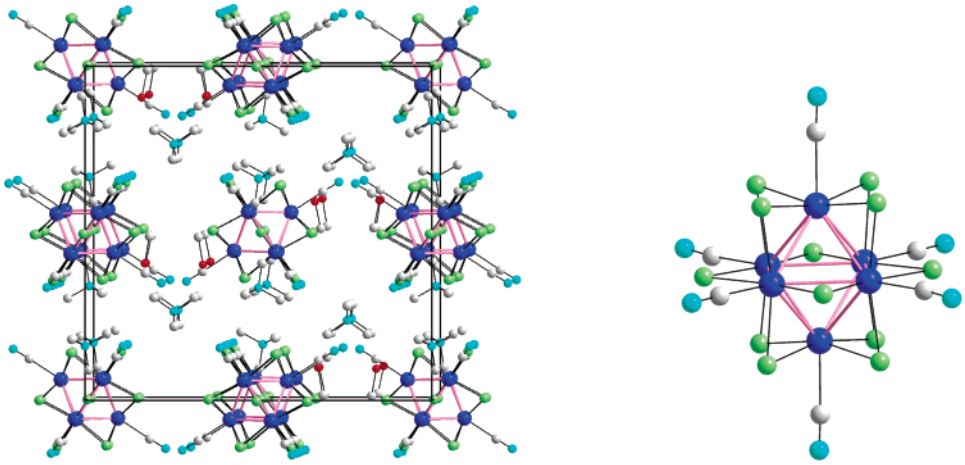

(a) **(b)**

Figure 1. (a) Projection of a unit cell of $(Me_4N)_4[Nb_6Cl_{12}(CN)_6]\cdot 2MeOH$ (**1**) along the crystallographic ***a*** axis. (b) Structure of the 16-electron cluster anion $[Nb_6Cl_{12}(CN)_6]^{4-}$ in $(Me_4N)_4[Nb_6Cl_{12}(CN)_6]\cdot 2MeOH$ (**1**). Blue, green, cyan, red, and light gray represent Nb, Cl, N, O, and C atoms, respectively. Hydrogen atoms are omitted for clarity. Selected bond distances (Å) and bond angles (deg): Nb−Nb 2.925(1), Nb−Cl 2.471(1), Nb−C 2.286(8), C−N 1.14(1) Å; Nb−C−N 177.9(7)°.

species and $[Mn(salen)]^+$ are critical for the formation of **3**, which was found to rapidly lose solvent when exposed to air at room temperature and quickly decayed to form an amorphous dark brown material.

Crystal Structures. *$(Me_4N)_4[Nb_6Cl_{12}(CN)_6]\cdot 2MeOH$ (1).* The structure of **1** is based on discrete $[Nb_6Cl_{12}(CN)_6]^{4-}$ cluster units held together by $(Me_4N)^+$ counterions and methanol solvent molecules (Figure 1a). The $[Nb_6Cl_{12}(CN)_6]^{4-}$ cluster anion is centrosymmetric and consists of an octahedral Nb_6 cluster coordinated by twelve edge-bridging chlorine ligands and six cyanide ligands located at the apical positions (Figure 1b). The mean intracluster bond lengths (Nb−Nb = 2.927(4) and Nb−Cl = 2.464(7) Å) are close to those found in other compounds containing $[Nb_6Cl_{12}(CN)_6]^{4-}$[8g,8i] and are within the standard deviations of those found in $Li_2Nb_6Cl_{16}$[16] from which the cluster $[Nb_6Cl_{12}]^{2+}$ was excised (Nb−Nb, 2.919(6) Å; Nb−Cl^i: 2.46(2) Å) indicating that the apical ligand and the counterions have negligible or no effect on the $[Nb_6Cl_{12}]^{2+}$ cluster core. In contrast, the Nb − Nb intracluster bond lengths are much shorter than those found in the 15-electron precursor $(Me_4N)_3[Nb_6Cl_{18}]\cdot 2MeCN$ containing $[Nb_6Cl_{12}]^{3+}$ with Nb−Nb = 2.983(5) Å, indicating that the electronic structure is the most important factor affecting these bond lengths. The mean bond lengths Nb−C = 2.282(1) and C≡N = 1.131(6) Å are similar to those found for other compounds containing the anionic $[Nb_6Cl_{12}(CN)_6]^{4-}$cluster species, and close to those observed for other niobium cyanide compounds.[8g,8i,17] The C≡N bond lengths are also virtually the same as those in cyanoxychlorides while Nb−C are slightly shorter. For example, the bond distances of C≡N and Nb−C in $(Me_4N)_5[Nb_6Cl_9O_3(CN)_6]\cdot 4H_2O$[8f] are 1.139(17) and 2.31(3) Å, respectively.

(16) Bajan, B.; Meyer, H. J. *Z. Anorg. Allg. Chem.* **1997**, *623* (5), 791−795.

(17) (a) Laing, M.; Gafner, G.; Griffith, W. P.; Kiernan, P. M. *Inorg. Chim. Acta* **1979**, *33*, L119. (b) Hursthouse, M. B.; Galas, A. M. *J. Chem. Soc., Chem. Commun.* **1980**, 1167. (c) Fedin, V. P.; Kalinina, I. V.; Virovets, A. V.; Podberezskaya, N. V.; Neretin, I. S.; Slovokhotov, Yu L. *Chem. Commun.* **1998**, 2579.

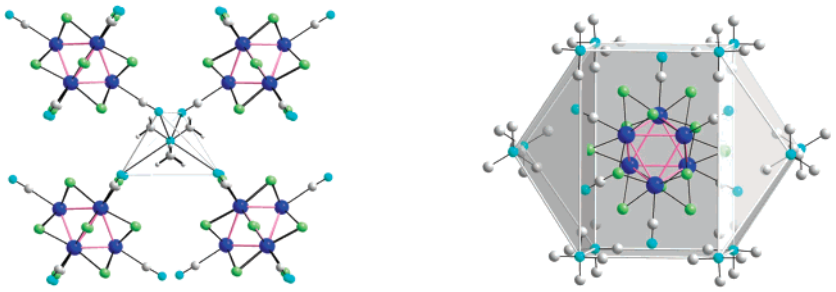

(a) **(b)**

Figure 2. (a) Projection showing the tetrahedral coordination environment of N4 in $[Me_4N]^+$ by four cyanides from four different cluster units. (b) Distorted hexagonal prism environment of the cluster $[Nb_6Cl_{12}(CN)_6]^{4-}$.

Table 2. Selected Mean Bond Lengths (Å) and Angles (deg) for $(Me_4N)_4[Nb_6Cl_{12}(CN)_6]\cdot 2MeOH$ (1), $(Me_4N)_2[Mn(salen)]_2[Nb_6Cl_{12}(CN)_6]$ (2), and $(Et_4N)_2[Mn(salen)(MeOH)]_2[Nb_6Cl_{12}(CN)_6]\cdot 2MeOH$ (3), and Comparison to Those Found in $(Me_4N)_2[MnNb_6Cl_{12}(CN)_6]$[8i]

	1	2	3	$(Me_4N)_2[MnNb_6Cl_{12}(CN)_6]$[8i]
Nb−Nb	2.927(4)	2.924(6)	2.934(6)	2.939(3)
Nb−Cl^i	2.464(7)	2.460(8)	2.465(8)	2.468(3)
Nb−C	2.282(1)	2.279(7)	2.286(14)	2.27(2)
C≡N	1.131(6)	1.133(4)	1.144(2)	1.16(3)
Nb−C≡N	178.3(6)	175.1(3)	176.7(5)	180.0
Mn−N_{CN}		2.233(3), 2.365(3)	2.295(3)	2.24(2)
Mn−C≡N_{CN}		144.2(3), 155.0(3)	157.2(3)	180.0
Mn−N≡C		173.3(1)		180.0

The Nb−C≡N is almost linear (178.3(6)°) and is within the range observed in other niobium cyanochloride cluster compounds.

The unit cell contains two crystallographically unique $[Me_4N]^+$ cations (N3 and N4). N3 is surrounded by two cyanide ligands (N2) from two different clusters and a methanol solvent molecule at a distance of 3.8 Å forming a distorted trigonal pyramid. The N4 ammonium ion is located in a distorted tetrahedral environment formed of four cyanide ligands from four different clusters (two N1 and two N2) at a distance less than 4 Å between N4 and N_{CN} (Figure 2a). The cluster unit is located in a distorted hexagonal prism (the pseudo 6-fold rotation axis is aligned along the *b* axis) formed by 12 $[Me_4N]^+$ cations (eight N4 and four N3) at a distance of less than 4 Å from the nitrogen end of the cyanide ligands (Figure 2b). In addition, each cluster is surrounded by two disordered MeOH which are hydrogen bonded to the cyanide ligand N1, ($O_{MeOH}\cdots N1_{CN}$ = 2.86(2) Å). Important bond lengths and angles are listed in Table 2.

$(Me_4N)_2[Mn(salen)]_2[Nb_6Cl_{12}(CN)_6]$ (**2**). Crystal structure analysis revealed **2** to be a layered material, in which $[Nb_6Cl_{12}(CN)_6]^{4-}$ and $[Mn(salen)]^+$ are linked by cyanide ligands to form anionic layers $\{[Mn(salen)]_2[Nb_6Cl_{12}(CN)_6]\}^{2-}$ parallel to the *(bc)* crystallographic plane (Figure 3a). The layers are interleaved by $(Me_4N)^+$ ions which serve as charge compensating ions. The cluster unit consists of the $(Nb_6Cl_{12})^{2+}$ cluster core with six additional cyanide ligands located in apical positions as found in the precursor **1**. Each cluster in **2** is linked to four $[Mn(salen)]^+$ through four cyanide ligands located in the equatorial plane forming Nb−CN−Mn−NC−Nb linkages in which the carbon end of the cyanide ligand connects to the niobium atom and the nitrogen end connects to the manganese center. Each $[Mn(salen)]^+$ is trans-coordinated by two N_{CN} from two different cluster units. The two remaining cyanide ligands are located in trans positions and point toward the interlayer spacing (Figure 3b). The layers stack along the crystallographic ***a*** axis in a staggered fashion with neighboring layers related to each other by ***b*** glide plane.

The mean bond lengths of Nb−Nb (2.924(6) Å) and Nb−Cl^i (2.460(8) Å) match those found for the cluster unit in **1** (2.927(4) and 2.464(7) Å for (**1**), respectively). The Nb−C interatomic distances 2.279(7) Å are not significantly different from those found in **1** (2.282(1) Å). The C≡N bond lengths and Nb−C≡N bond angles of the cyanide ligands that act as linkers (1.134(4) Å and 174.7(3)°, respectively) are nearly the same as those of the terminal cyanide ligands pointing to the interlayer spacing (1.131(5) Å, 175.3(4)°). This is confirmed by the presence of only one slightly broad IR absorption band at 2134 cm^{-1}. In contrast, two IR absorption bands are observed for C≡N in the 2-D network of $(Et_4N)[Mn(salen)_2Fe(CN)_6]$[18] and in the rhenium telluride cluster-based network $[Mn(salen)]_{4n}[Re_6Te_8(CN)_6]_n$.[12a] The Mn metal center is octahedrally coordinated by two O and two N atoms from *salen* ligand in an almost planar fashion, and two trans N_{CN} from two cluster units. The mean Mn−O_{salen} and Mn−N_{salen} bond lengths (1.878(2) and 1.98(2) Å, respectively) are similar to those found in $[Mn(salen)Cl]\cdot H_2O$,[19] but significantly smaller than those observed in $[Mn(II)(salen)(py)_2]$[20] (2.04(2) and 2.22(1) Å). Two Mn−N_{CN} bond lengths are observed, 2.233(4) and 2.365(3) Å, with the corresponding Mn−N−C bond angles 155.0(3)° and 144.2(3)°. These values are comparable to those found in the 1-D

(18) Miyasaka, H.; Ieda, H.; Matsumoto, N.; Sugiura, K. I.; Yamashita, M. *Inorg. Chem.* **2003**, *42*, 3509.
(19) Martínez, D.; Motevalli, M.; Watkinson, M. *Acta Crystallogr.* **2002**, *C58*, m258.
(20) Srinivasan, K.; Michaud, P.; Kochi, J. K. *J. Am. Chem. Soc.* **1986**, *108*, 2309.

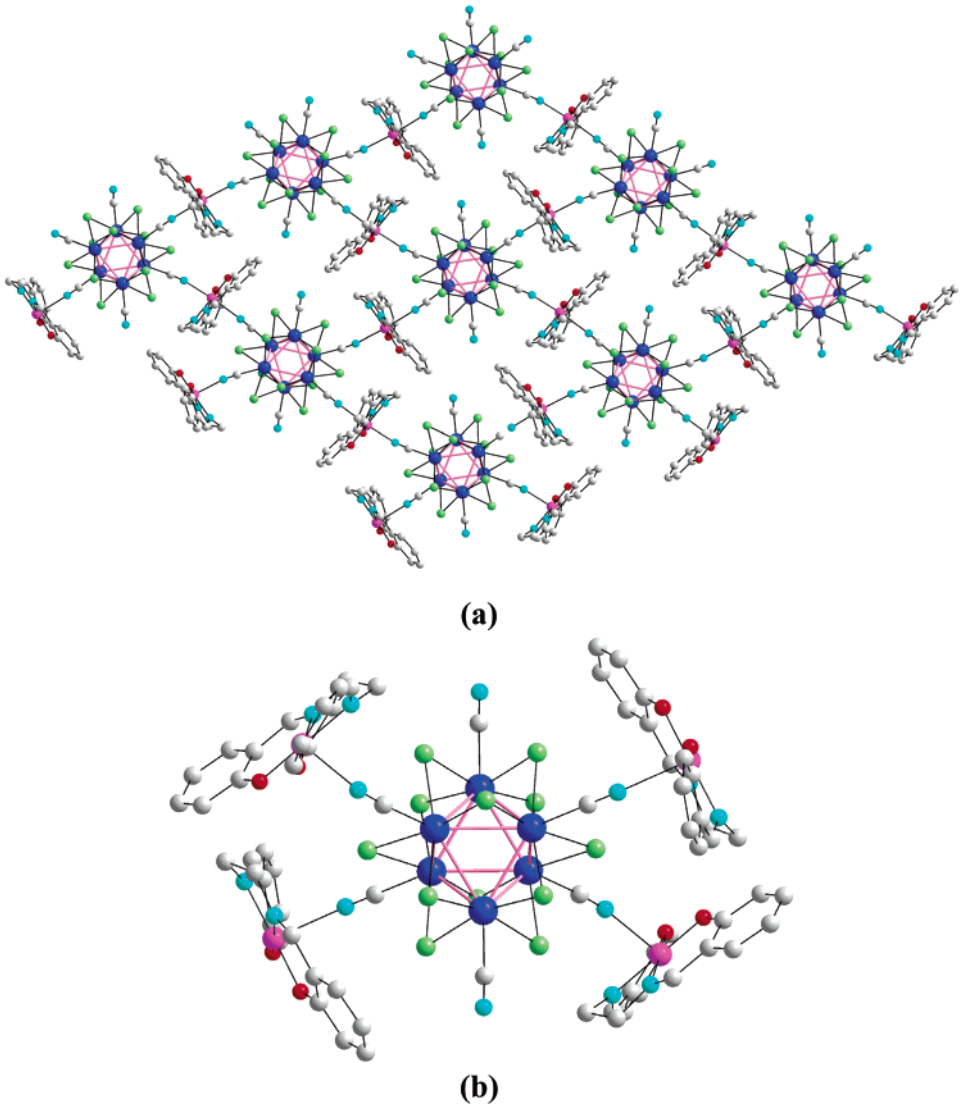

Figure 3. (a) Projection along [100] of one layer in $(Me_4N)_2[Mn(salen)]_2[Nb_6Cl_{12}(CN)_6]$ (**2**). Purple, blue, green, cyan, red, and light gray represent Mn, Nb, Cl, N, O, and C atoms, respectively. Hydrogen atoms and templates are omitted for clarity. (b) The secondary building unit in (**2**) showing the connectivity between the $[Nb_6Cl_{12}(CN)_6]^{4-}$ cluster unit and the $[Mn(salen)]^+$ complex.

compound [Mn(*salen*)CN][21] (2.25(3) Å and 147(3)°). The distance between the nearest Mn metal centers in adjacent layers is 8.196(1) Å. Selected bond distances and bond angles are listed in Table 2.

*$(Et_4N)_2[Mn(salen)(MeOH)]_2[Nb_6Cl_{12}(CN)_6]\cdot 2MeOH$ (**3**).* Compound **3** features a 1D framework built of $[Nb_6Cl_{12}(CN)_6]^{4-}$ cluster units and $[Mn(salen)]^+$ metal complexes connected to each other through cyanide ligands (Figure 4a). Each cluster shares two trans cyanide ligands with the metal complex leading to the formation of {Mn−(NC)$[Nb_6Cl_{12}(CN)_4]$(CN)Mn} trimeric assemblies, that can be considered as secondary building unit (SBU) (Figure 4b). In addition to the two oxygen and two nitrogen atoms from the *salen* ligand, the Mn center is trans- coordinated by one N_{CN} from the cyanide ligand of the cluster unit and one MeOH solvent molecule. The O_{MeOH} of the coordinated MeOH forms hydrogen bonding with the N_{CN} from neighboring SBU ($O_{MeOH}-N_{CN}$ = 2.720(4) Å, bond angle O−H···N = 169-(5)°) leading to the formation of anionic chains $\{[Mn(salen)(MeOH)]_2[Nb_6Cl_{12}(CN)_6]\}^{2-}$ along the crystallographic ***a*** axis. The strength of this hydrogen bonding is comparable to that observed in organic polymeric chains.[22] The chains are related to each other by the ***c*** glide plane. MeOH and $(Et_4N)^+$ are located between the chains.

The mean bond lengths Nb−Nb = 2.934(6) and Nb−Cl = 2.465(8), Nb−C = 2.286(14), and C≡N 1.144(2) Å are the same as those found in the cluster unit in **1** and **2**, confirming the presence of the cluster $[Nb_6Cl_{12}(CN)_6]^{4-}$ with VEC = 16. IR spectra show only one band at 2131 cm^{-1} corresponding to CN bond stretch. This is surprising since three kinds of cyanide ligands are present in the framework of **3**: one acts as linker between the cluster and Mn, one forms strong hydrogen bonding with the coordinated MeOH, and one forms strong hydrogen bonding with noncoordinating MeOH with $N_{CN}\cdots O$ = 2.90(1) Å. The differences between these CN ligands are probably not large enough for the C≡N

(21) Matsumoto, N.; Sunatsuki, Y.; Miyasaka, H.; Hashimoto, Y.; Luneau, D.; Tuchagues, J. P. *Angew. Chem., Int. Ed.* **1999**, *38*, 171.

(22) (a) Hökelek, T.; Zülfikaroğlu, A.; Bati, H. *Acta Crystallogr.* **2001**, *E57*, 01247. (b) Büyükgüngör, O.; Hökelek, T.; Bati, H. *Acta Crystallogr.* **2003**, *E59*, 0883.

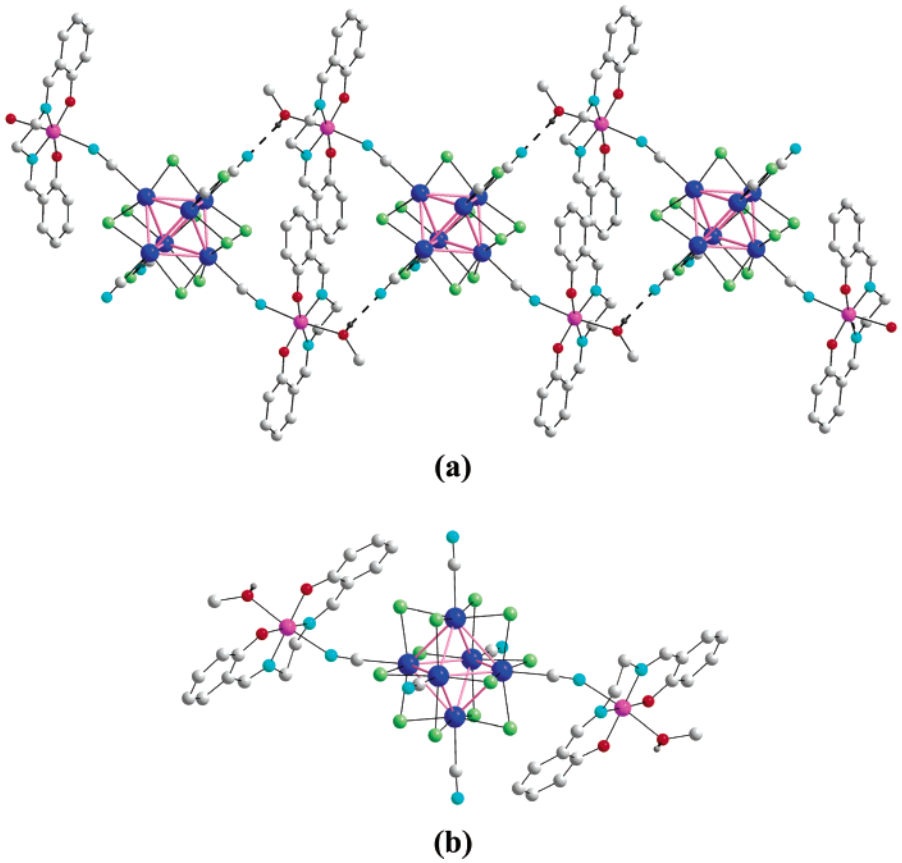

Figure 4. (a) Anionic chain along the ***a*** axis. Purple, blue, green, cyan, red, and light gray represent Mn, Nb, Cl, N, O, and C atoms, respectively. The dashed lines represent hydrogen bonding. (b) Two *trans*-CN ligands of $[Nb_6Cl_{12}(CN)_6]^{4-}$ coordinate to two [Mn(*salen*)(MeOH)]$^+$ to form trimeric units [Mn−(NC)[$Nb_6Cl_{12}(CN)_4$](CN)Mn]. The small medium gray balls represent hydrogen atoms that participate in hydrogen bonding. All other hydrogen atoms are omitted.

stretches to be resolved. The Mn−O_{salen} = 1.881(3) Å and Mn−N_{salen} = 1.992(3) Å bond lengths are nearly the same as those found for **2**, while the Mn−N_{CN} = 2.295(3) Å bond length is between the two values observed in **2.** Selected bond distances and bond angles are listed in Table 2.

The structures of **2** and **3** are different from those of the two previously reported compounds composed of [Mn(*salen*)]$^+$ and cyano-rhenium clusters as building units, $[Mn(salen)]_{4n}[Re_6Te_8(CN)_6]_n$ which has a 2D framework and $Na[Mn(salen)]_3[Re_6Se_8(CN)_6]$ which is characterized by a 3D network.[12] In contrast to the rhenium based compounds in which all six cyanide ligands connect the cluster to the manganese complex, in **2** and **3** only four and two cyanide ligands serve as linkers between the $[Nb_6Cl_{12}]^{2+}$ cluster and the [Mn(*salen*)]$^+$ complexes. The 2D framework of $[Mn(salen)]_{4n}[Re_6Te_8(CN)_6]_n$ differs from that observed in **2** in that two cyanide groups coordinate to nonbridging [Mn(*salen*)]$^+$ leading to the formation of neutral framework. In the 3D compound $Na[Mn(salen)]_3[Re_6Se_8(CN)_6]$ all six cyanide groups coordinate to bridging Mn(*salen*)$^+$ to create a 3D framework. These structural differences might be due to the following factors: (*i*) the edge-capped $[Nb_6Cl_{12}(CN)_6]^{4-}$ clusters are larger compared to the face-capped cluster $[Re_6X_8(CN)_6]^{4-}$ (X = Se, Te); (*ii*) The sizes of $(Me_4N)^+$ and $(Et_4N)^+$ counterions used in the preparation of **2** and **3** are much bigger than that of Na^+, and (*iii*) the solvent systems are different.

Magnetic Properties. The magnetic susceptibility data for **2** over the temperature range 2−300 K (shown in Figure 7 in the Supporting Information) can be well described by the Curie−Weiss relation, $\chi(T) = \chi_0 + C/(T - \theta)$, with C = 13.387 emu K mol^{-1}, θ = −2.225 K, and $\chi_0 = 2.18 \times 10^{-4}$emu mol^{-1}. At room temperature, **2** displays effective magnetic moment of 7.34μ_B, which is close to the spin-only effective moment of high-spin Mn^{3+} ions (6.94μ_B). No evidence for magnetic ordering was observed in temperatures down to 2 K. Meaningful magnetic susceptibility measurements could not be carried on **3** due to the compound's fast loss of crystallinity in air.

Thermal Stability. The stability of compound **2** was investigated by thermal analysis. Two distinct weight loss steps were observed. The first (35.2%) occurred in the temperature range 330−470 °C and might correspond to simultaneous loss of $(Me_4N)^+$ and *salen* ligand (ca 35.3%). The second weight loss (8.4%) occurred above 600 °C and is consistent with loss of all cyanide ligands (ca 8.1%). X-ray powder diffraction shows collapse of the framework and formation of another phase that has not yet been identified.

Conclusion

The octahedral cyano-chloride cluster $[Nb_6Cl_{12}(CN)_6]^{4-}$ and the metal complex [Mn(*salen*)]$^+$ were employed in the preparation of cluster-based hybrid inorganic−organic extended frameworks. The high-spin d^4 electronic configuration of Mn(III) introduces paramagnetic properties into the resulting materials, however no long-range magnetic order has been observed in these

materials. The tetraalkylammonium species seem to play an important role in the structural properties of the resulting frameworks. Thus, $(Me_4N)^+$ leads to the formation of the 2D framework in **2**, while a relatively larger $(Et_4N)^+$ leads to 1D coordination polymer in which two of the six cyanide ligands coordinate to two $[Mn(salen)]^+$ metal complexes, and the remaining four CN ligands form hydrogen bonding with either coordinated or free solvent molecules to form chains. The formation of **2** seems to be independent of the precursors' concentrations, while the concentration of both species is critical to the formation of **3**. The formation of **2** is independent of the solvent used since it can also be obtained using MeCN as the solvent, while MeOH plays an important role in the formation of **3** since hydrogen bonding between the cyanide ligands and coordinated and noncoordinated solvent molecules is responsible for the formation of the 1D framework in **3**. Attempts to grow crystals using Na^+ or PPh_4^+ as countercations were not successful. Investigations of using different templates, different predesigned metal complexes, and different solvents are continuing and should lead to better understanding of the conditions controlling the formation of cluster-based hybrid inorganic−organic materials.

Acknowledgment. This material is based upon work supported by the National Science Foundation under Grant DMR-0070915. Acknowledgment is made to the donors of the Petroleum Research Fund, administered by the American Chemical Society, ACS-PRF#36080-AC5 for partial support of this work. This material is based upon work supported by the National Science Foundation under Grant No. 0305245. We thank Prof. Tim Hughbanks of Texas A&M University for his helpful discussions and advice. We thank Prof. Paul A. Maggard from the North Carolina State University for his assistance with magnetic data measurements and X-ray powder diffraction measurements.

Supporting Information Available: IR spectra of compounds **2** and **3**; TGA of compound **2** under nitrogen and magnetic susceptibility data plot of compound **2**; PXRD patterns of the materials obtained after TGA of compound **2** (after 600 °C); comparison of three PXRD patterns of the materials obtained after TGA of compound **2** after 600 °C, **2** after 900 °C, and $(Me_4N)_2[MnNb_6Cl_{12}(CN)_6]$ after 600 °C (PDF). X-ray crystallographic files in CIF format of the three compounds reported. This material is available free of charge via the Internet at http://pubs.acs.org.

CM049007W